Investigating Tryptophan Quenching of Fluorescein Fluorescence under Protolytic Equilibrium

Denisio M. Togashi,* Boguslaw Szczupak, Alan G. Ryder, Amandine Calvet, and Muireann O'Loughlin

Nanoscale Biophotonics Laboratory, School of Chemistry and National Centre for Biomedical Engineering Science, National University of Ireland, Galway, Galway, Ireland

Received: September 12, 2008; Revised Manuscript Received: January 7, 2009

Fluorescein is one of most used fluorescent labels for characterizing biological systems, such as proteins, and is used in fluorescence microscopy. However, if fluorescein is to be used for quantitative measurements involving proteins then one must account for the fact that the fluorescence of fluorescein-labeled protein can be affected by the presence of intrinsic amino acids residues, such as tryptophan (Trp). There is a lack of quantitative information to explain in detail the specific processes that are involved, and this makes it difficult to evaluate quantitatively the photophysics of fluorescein-labeled proteins. To address this, we have explored the fluorescence of fluorescein in buffered solutions, in different acidic and basic conditions, and at varied concentrations of tryptophan derivatives, using steady-state absorption and fluorescence spectroscopy, combined with fluorescence lifetime measurements. Stern−Volmer analyses show the presence of static and dynamic quenching processes between fluorescein and tryptophan derivatives. Nonfluorescent complexes with low association constants (5.0−24.1 M^{-1}) are observed at all pH values studied. At low pH values, however, an additional static quenching contribution by a sphere-of-action (SOA) mechanism was found. The possibility of a proton transfer mechanism being involved in the SOA static quenching, at low pH, is discussed based on the presence of the different fluorescein prototropic species. For the dynamic quenching process, the bimolecular rate constants obtained (2.5−5.3 × 10^9 $M^{-1}s^{-1}$) were close to the Debye−Smoluchowski diffusion rate constants. In the encounter controlled reaction mechanism, a photoinduced electron transfer process was applied using the reduction potentials and charges of the fluorophore and quencher, in addition to the ionic strength of the environment. The electron transfer rate constants (2.3−6.7 × 10^9 s^{-1}) and the electronic coupling values (5.7−25.1 cm^{-1}) for fluorescein fluorescence quenching by tryptophan derivatives in the encounter complex were then obtained and analyzed.

1. Introduction

Widely applied in fluorescence imaging microscopy, the fluorophore-labeled protein can be used to rapidly and easily visualize many different biochemical pathways, which involve protein interactions, protein expression, trafficking, intracellular signaling events, and cellular location.[1,2] Many of the fluorophores used are designed to conjugate with specific amino acid residues or functional groups present in the target biomolecule. In many cases, the fluorophore is simply used as a contrast agent to show the location of the target biomolecule in a particular environment. However, for quantitative measurements of protein-surface interactions using techniques like Förster resonance energy transfer (FRET), fluorescence lifetime imaging (FLIM), or fluorescence correlation spectroscopy (FCS),[3−5] the possibility of changes in emission spectra, fluorescence intensity, or lifetime due to intramolecular or intermolecular factors can be significant and can adversely affect the interpretation of data. The photophysical parameters of a fluorophore are obviously dependent on various external environmental factors such as pH, polarity, temperature, ion concentration, membrane potential, and so forth. [2,6,7] However, fluorophore emission after conjugation (covalent or otherwise) to a macromolecule can be completely different from the free probe, under the same environmental conditions,[8−11] due to the possibility that the emission properties may be affected by the microenvironment of the binding site, primarily via non radiative mechanisms.[12−15] Of particular significance is the quenching interaction of specific amino acids in the protein, like tryptophan.[16−18]

Fluorescein and its derivatives are the most widely used family of fluorophores in biology.[2,6,7]They are easily excited, reasonably photostable, and have high fluorescence quantum yields.[2,6] In particular, they are widely used in fluorescence microscopy and FRET studies.[1,19] Unfortunately, fluorescein can exist in different species (prototropic forms) with dissimilar photophysical properties, depending on the environmental pH.[20−22] Fluorescein in aqueous solution can exist as cationic (FH_3^+), neutral (FH_2), monoanionic (FH^-), and dianionic (F^{2-}) species (Scheme 1), the concentrations of which are dependent on the pH.[20−22] Furthermore, the neutral form can exist as three different isomers: quinoid (Q), zwitterion (Z), and lactone (L) forms.[20a] Other environmental conditions such as ionic strength and temperature also have an impact on the equilibria.[20b,23]The pK_a values are normally determined from analysis of the electronic absorption spectra of fluorescein in an acid−base titration experiment. The direct determination of an accurate absorption spectrum for most of the individual prototropic species is unreliable, except for the dianion, because of the overlap between the individual spectral contributions in the absorption spectra. Therefore, to extract the individual

* To whom correspondence should be addressed. Tel.: +351(0)91495186. Fax: +351(0) 91 52 5700. E-mail: denisio.togashi@nuigalway.ie.

10.1021/jp808121y CCC: $40.75
Published on Web 03/02/2009

SCHEME 1: Ground State Fluorescein Protolytic Equilibria

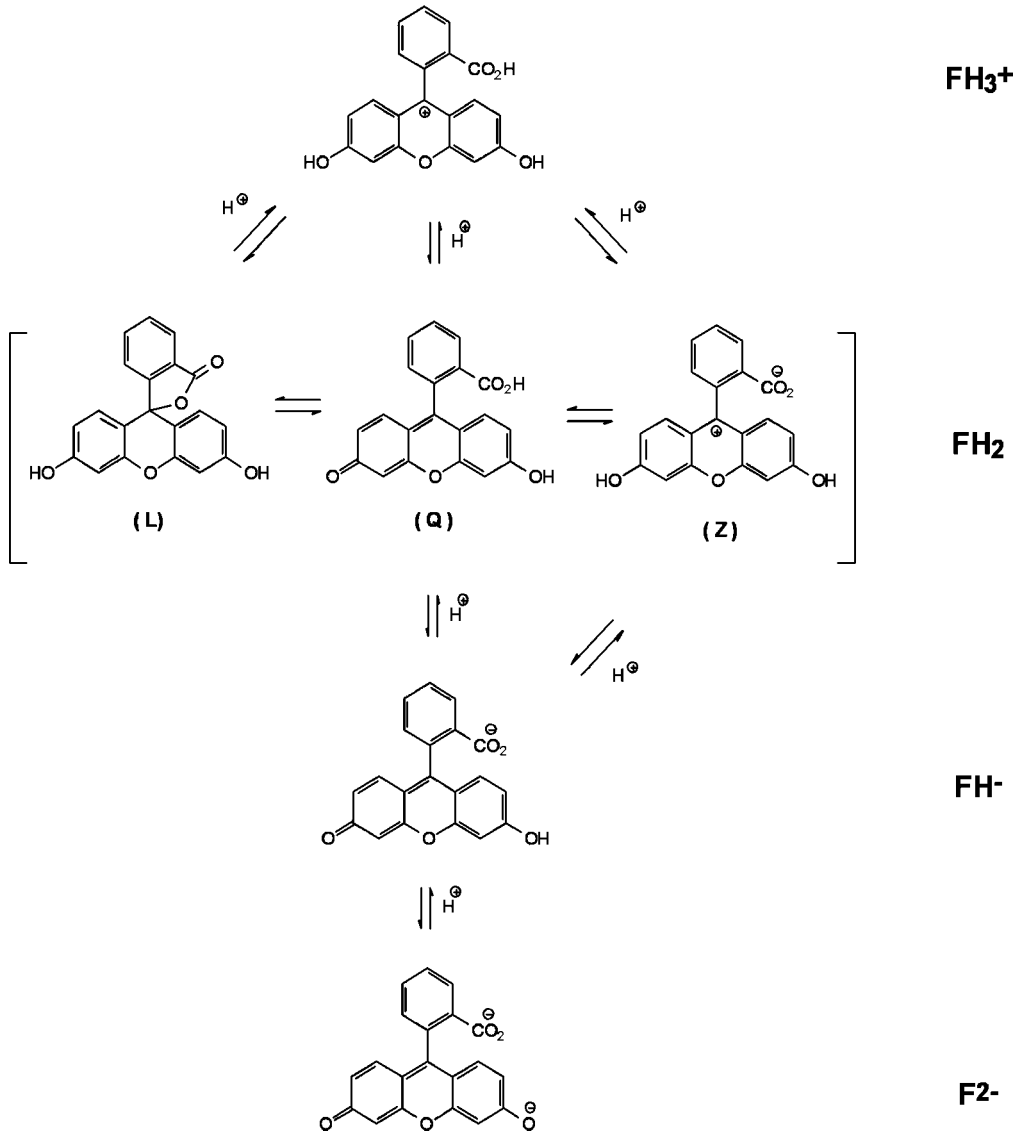

absorption spectra for pK_a measurements, one has to use a spectral resolution procedure, or a multispecies equilibrium model with the analysis of absorption changes at one or more wavelengths, or chemometric methods.[20,22] Different p$K_a$values have been reported because of the number of different approaches utilized. In general, the three pK_a values are in the range 2.00−2.25, 4.23−4.4, and 6.31−6.7.[20−23] Recently, these values were corrected by using activity coefficients and reported as pK_{a1} = 2.22, pK_{a2} = 4.34, and pK_{a3} = 6.68.[23]

Despite the fact that the majority of experimental observations reported in the literature are in agreement, there are some controversies related to the identity of the excited-state species and the interconversion between excited-state species.[20,21] Under alkaline conditions (pH >8), where the dianion is the dominant species in the ground state, the fluorescence spectral profile does not change with proton concentration. At acidic pH (∼1.5 to ∼5), where the dominant species of fluorescein in the ground-state are cationic, neutral, and monoanion forms, the profile of the fluorescence spectra is also always the same. However, at near neutral pH (between ∼5 and ∼8) where the neutral, monoanion, and dianion are present, one observes changes in the profile of the fluorescence spectrum.

It is in the analysis and interpretation of these observations that the two main questions arise: (i) the contribution and importance of different neutral forms of fluorescein to the fluorescence emission,[20] and (ii) the effect of phosphate buffers on the excited state of the monoanion and dianion.[20a−c,21] The first issue refers to the nature of the contribution to the measured fluorescence spectrum from the other species apart from the dianion, present at near neutral pH: this contribution is either composed of emission from both neutral and monoanion species (both species having very similar emission spectra),[20a,d] or the emission originates only from the monoanion.[20b,c] This controversy originates from the spectral analysis approach used in the different literature studies. One view is that, irrespective of the exact structure of the neutral form, the neutral species is always nonfluorescent.[20b,c] However, other studies show that the neutral fluorescein species, in aqueous solution, exists as a combination of lactone, quinone, and zwitterion forms.[20a] Only the quinone form is fluorescent with a quantum yield of 0.29, which is similar in magnitude to the quantum yield of the monoanion (0.36).[20a]

There is agreement in the literature that the fluorescence emission can be decomposed linearly into two spectra corresponding to the dianion and the nondianion forms for pH above ∼1.5. Also, a fast proton transfer equilibrium reaction occurs between pH ∼1.5 and ∼5, which means that there is a fast interconversion between the cationic, neutral, and monoanion

species during the excited-state lifetime. This conversion is estimated to be up to 85%.[20b,c] In the pH region above ~5, the conversion in the excited state between the nondianion species and the dianion does not occur in water or in low phosphate-buffer concentration. Therefore, under the physiological conditions encountered in most bioscience applications, the dianion is the predominant fluorescein species present, and it has a large absorption coefficient and high fluorescence quantum yield. It has been observed, however, that fluorescein emission can be quenched by amino acids.[16−18] A more detailed analysis of the amino acid quenching mechanism, which takes into account the presence of other prototropic species and structural effects (such as distance dependence of the quencher molecule), is still required for a comprehensive, quantitative understanding of fluorescein photophysics in proteins.

In this article, we investigate in detail the fluorescence quenching of hydrolyzed fluorescein diacetate (FDAH) by tryptophan derivatives (or indole core compounds) by using UV−vis absorption and fluorescence emission and lifetime spectroscopy. The quenching process was studied over a pH ranged values to ascertain the effect of the presence of different prototropic species. The Stern−Volmer constants and quenching rate constants were obtained. In addition, electron transfer parameters (ET) using diffusion Debye−Smoluchowski and ET Marcus models were applied to extract distance dependence data from the fluorescence quenching analysis. Our particular interest is to obtain baseline photophysical data that can be applied to the detailed study of the photophysics of fluorescein conjugated to proteins used for exacting quantitative fluorescence microscopy applications.

2. Experimental Procedures

Materials. Fluorescein (F), Fluorescein Diacetate (FDA), Tryptamine (TrpA), and *N*-Acetyl-DL-tryptophan (AcTrp) were obtained from Sigma-Aldrich. The pH 2.0, 5.0, and 11.0 buffers with estimated ionic strengths of 0.07 M, 0.31 M, and 0.10 M respectively were obtained from FIXANAL. The pH 7.4 buffer was made up using PBS tablets (Fluka) and had an ionic strength of 0.16 M.[24] All reagents were used as received without further purification. All aqueous solutions were made up with deionized water from a Milli-Q Millipore system.

Apparatus. Absorption spectra were recorded with a PerkinElmer Lambda 950 UV−vis spectrophotometer in a 2 mm path length quartz cell, with the sample held at room temperature (21 °C). Fluorescence spectra were made using a Cary Eclipse Fluorescence Spectrophotometer (Varian) and spectra were corrected by the correction curves provided by the manufacturer. Magic-angle fluorescence decays were recorded using a Time Correlated Single Photon Counting system (Fluotime 200, Picoquant GmbH). The excitation at 440 nm was a pulsed laser diode (LDH-440, Picoquant GmbH) at 5 MHz, and the fluorescence was detected at 520 nm. Typical full widths at half-maximum obtained for instrument response function are on the order of a hundred picoseconds and were obtained using an aqueous Ludox solution. All measurements were stopped at a count of 20 000 in the time channel of maximum intensity. Samples within micromolar concentration were held in a 1 mm path length quartz cuvette using front-surface excitation geometry to reduce as much as possible any inner-filter effects.

FDA Hydrolysis. FDA (5.6 mg) was dissolved in 2 mL methanol and then 1 mL of 1 M NaOH was added. The solution was then neutralized with approximately 83 μL of (37%) hydrochloric acid. The product of FDA hydrolysis is fluorescein at a final concentration of 2.9 mM, hereafter called FDAH.

Fluorescence Quantum Yields. Fluorescence quantum yields (Φ_f) were determined using fluorescein in NaOH (0.1 M), $\Phi_f = 0.72$,[25] as a standard, after applying necessary corrections for the refractive index of the medium. FDAH concentrations of ~3 μM were used in all fluorescence measurements to keep the absorption below 0.06. The error in the estimation of Φ_f is ±10%. All of the fluorescence intensity measurements were carried out on nondeaerated samples at room temperature.[25]

Quenching Experiments. Because of solubility issues in buffered solutions, at pH 5.0, 7.4, and 11.0, stock solutions of 0.1 M AcTrp in 0.2 M NaOH were first prepared. Solutions of AcTrp at pH 5.0, 7.4, and 11.0 were generated by carefully monitoring, using a pH meter, the addition of small volumes of concentrated HCl. The final ionic strength of the stock solutions was ~0.2 M. Tryptamine hydrochloride (TrpA) 0.1 M stock solutions were prepared in the respective buffered solutions pH 2.0 and 5.0 and verified using a pH meter. For different quencher concentrations, a corresponding aliquot of a stock solution was taken and diluted with the buffer solution of respective pH. A final concentration of approximately 5 μM hydrolyzed FDA was then used in all Stern−Volmer experiments.

Data Analysis. Lifetime data were analyzed using the *FluoFit*, version 4.1 (Picoquant) software package. The intensity averaged lifetime is calculated by $\tau_{av} = \sum f_i\tau_i$, where $f_i = a_i\tau_i / \sum a_i\tau_i$ is the contribution factor of the i^{th} exponential term, with a pre-exponential a_i and decay time τ_i. The GOF was assessed by having a χ^2 value of less than 1.2 and a residual trace that was symmetric about the zero axes. The lifetime errors, which were typically less than 0.05 ns were calculated by using the error surface analysis provided by the software package with 99% probability on the χ^2 value.

3. Results and Discussion

3.1. FDAH Prototropic Species. There were no significant differences in the steady-state absorption (part A of Figure 1) or fluorescence (part B of Figure 1) spectra of FDAH compared to the pure fluorescein standard recorded at different pH. This indicates that the FDA to FDAH hydrolysis process does not change the relative ion concentration for the fluorescein prototropic species. At pH 2.0, the absorption spectrum (λ_{max} = 435 nm) corresponds to the cationic form; however the presence of a shoulder near 480 nm indicates that some of the neutral form is also present, which is in agreement with reported studies.[20] Analysis of the prototropic equilibria pK_a values (pK_{a1} = 2.22, pK_{a2} = 4.34, and pK_{a3} = 6.68)[23] indicates that there is no significant contribution from the anionic species to the ground-state equilibrium at pH 2.0 (Table 1). However, the FDAH fluorescence spectrum obtained at pH 2.0 is very similar to the fluorescence spectrum of the anionic species. This is because of the fast cationic ↔ neutral ↔ monoanion equilibrium that is established in the excited state.[20,21] Therefore, irrespective of whether the cationic or neutral form is excited, the species responsible for emission at pH 2.0 is the monoanion.

The main prototropic forms in the ground-state equilibrium of FDAH at pH 5.0 and 7.4 are the monoanion (80%) and dianion (84%), respectively. Both forms contribute to the absorption spectra, for example the monoanion broadening the band at 490 nm (part A of Figure 1) at pH 7.4. Both species also contribute to the fluorescence spectra, for example the dianion fluorescence overlaps the monoanion emission at pH 5.0 (part B of Figure 1). The absorption and fluorescence spectra at pH 11.0 correspond almost entirely to the dianion.[20−22]

The existence of different prototropic species with a high degree of emission spectral overlap, and the presence or absence

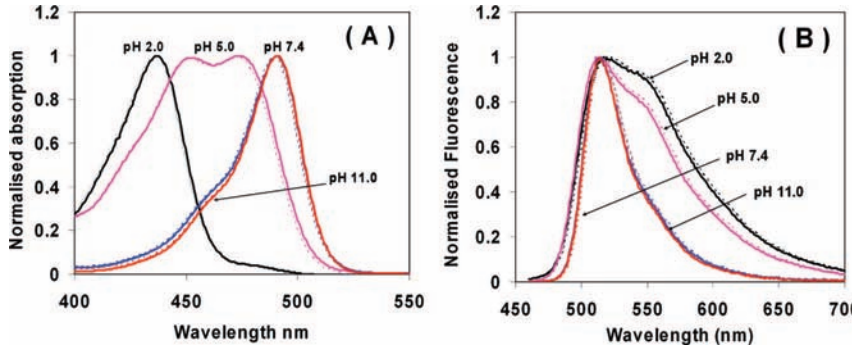

Figure 1. Normalized absorption (A) and fluorescence (B) spectra for FDAH (solid lines) and fluorescein (dashed lines) at different pH and in buffered solutions. Note that the fluorescein absorption and fluorescence spectra have been offset by 1 nm on the wavelength scale for clarity. Otherwise, all spectra would perfectly overlap the corresponding absorption and fluorescence spectra of FDAH.

TABLE 1: Percentage Contribution of Fluorescein Prototropic Species and Photophysical Parameters for FDAH and Fluorescein (in brackets) under Different Experimental Conditions

pH	C, N, M, D (%)[a]	Φ_f	τ_f /ns
2.0	68, 32, 0, 0	0.20 (0.19)	2.91 (2.91)
5.0	0, 18, 80, 2	0.23 (0.25)	3.53 (3.51[b])
7.4	0, 0, 16, 84	0.58 (0.59)	4.01 (3.97)
11.0	0, 0, 0, 100	0.63 (0.64)	4.04 (3.97)

[a] C (cation), N (neutral), M (anion), and D (dianion). [b] As biexponential: 4.00 ns (fixed) and 3.37 ns with fractional intensity of 23% and 77%, respectively.

of excited-state proton transfer equilibria, explain the large differences in the reported absolute fluorescence quantum yields for the different prototropic species ($\Phi_{FH_{3+}} = 0$, 0.39 (0.9−1.0), $\Phi_{FH_2} = 0-0.30$, $\Phi_{FH-} = 0.26-0.37$, and $\Phi_{F_{2-}} = 0.93$). [20−22]

3.2. Interaction between FDAH and Tryptophan Derivatives. The UV−vis spectra of buffered solutions of FDAH are affected by the presence of tryptophan derivatives. In parts A (pH 2.0) and B (pH 5.0) of Figure 2, there are absorption contributions from TrpA due to the high concentrations used. Conversely, the AcTrp absorption in alkaline media (parts C and D of Figure 2) is weaker than that observed for TrpA in acid media. Thus, this extra contribution in the absorption spectra can mask significant FDAH interaction effects with tryptophan. Fortunately, this can be rectified by subtracting the absorption spectra of the corresponding pure solutions of the tryptophan derivatives at the same concentration, giving the FDAH absorption corrected spectra (parts A'−D' of Figure 2).

The corrected FDAH absorption spectra show very small but consistent changes in the main absorption band, first a reduction in intensity, and second a red shift, with $\lambda_{max} = 436$ nm at pH 2.0, 452 nm at pH 5.0, 490 nm at pH 7.4, and 491 nm at pH 11. Furthermore, isobestic points were detected at approximately 448, 485, 498, and 496 nm for pH 2.0, 5.0, 7.4, and 11.0, respectively. At pH 5.0 (part B' of Figure 2), the small variations of absorption values at the maxima (<0.002) made it very difficult to observe the isobestic point. However, increasing the FDAH concentration (2-fold) and path length (to 10 mm) enabled observation of the isobestic point. These changes in the absorption spectra are due to the formation of a weak association complex.

At pH 2.0 and 5.0, the charge of the main TrpA species is positive because its $pK_a = 9.3$.[26a] Assuming similar pK_a values for AcTrp and tryptophan ($pK_{a1} = 2.38$ and $pK_{a2} = 9.39$),[26b] the charge of the main AcTrp species at pH 5.0 and 7.4 is zero, whereas at pH 11 AcTrp with a −1 charge is dominant. If one considers the charges of the interacting species, then an electrostatic interaction may be responsible for formation of the weak complex observed in the absorption spectra. It is only at pH 5.0 where there are favorable conditions for complex formation because TrpA is positively charged and the main fluorescein form is negatively charged. In fact, the measured association constant for the complex reaches the highest value at pH 5.0 (vide infra). Under the other pH conditions studied, complex formation is much less likely because of unfavorable charges. However, the repulsive/attractive electrostatic interactions can be reduced in solutions of high ionic strength due to an ion screening process.[27]

Figure 3 shows the fluorescence spectra of FDAH in the presence of tryptophan derivatives. The fluorescence intensity maxima are found at 516 nm (554 nm, shoulder), 514 nm (553 nm, shoulder), 516 nm, and 516 nm for pH 2.0, 5.0, 7.4, and 11.0, respectively. In contrast to the absorption spectra and despite the decrease of intensity due to quenching, the fluorescence spectra do not show any changes in profile and are identical to those as shown in part B of Figure 1. Furthermore, the unchanged spectral shape of FDAH at all pHs studied is an indication that the presence of high concentrations of tryptophan derivatives does not affect the excited-state equilibrium between the prototropic forms, that is the presence of quencher does not affect the proton transfer process that may occur in the excited state.

3.3. FDAH Fluorescence Quantum Yield and Lifetime. The fluorescence quantum yields and fluorescence lifetimes for FDAH obtained at different pH (Table 1) are similar to those obtained for the fluorescein standard under the same experimental conditions, indicating that the hydrolysis process did not affect the photophysical properties of the fluorescein moiety. All of the fluorescence decays could be fitted to a single exponential function, which is expected if the contribution of one or two anionic species in the excited state is very small at the emission wavelength of 520 nm for the pH 2.0, 7.4, and 11.0. However, at pH 5.0 one would have expected a second lifetime component due to the presence of significant quantities of both monoanion and dianion FDAH prototropic forms as indicated by the emission spectrum (part B of Figure 1).

If one assumes that the fluorescence emission at pH 11.0 originates only from the dianion and that the pH 2.0 fluorescence emission is due only to the monoanion, then the contribution of monoanion fluorescence to the fluorescence spectrum at pH 5.0 can be calculated using multilinear regression of the pH 2.0 and 11.0 fluorescence spectra, obtained at the same concentration.[20] Figure 4 shows that a reasonable fit is obtained, and one can ascribe the observed deviations to the fact that the

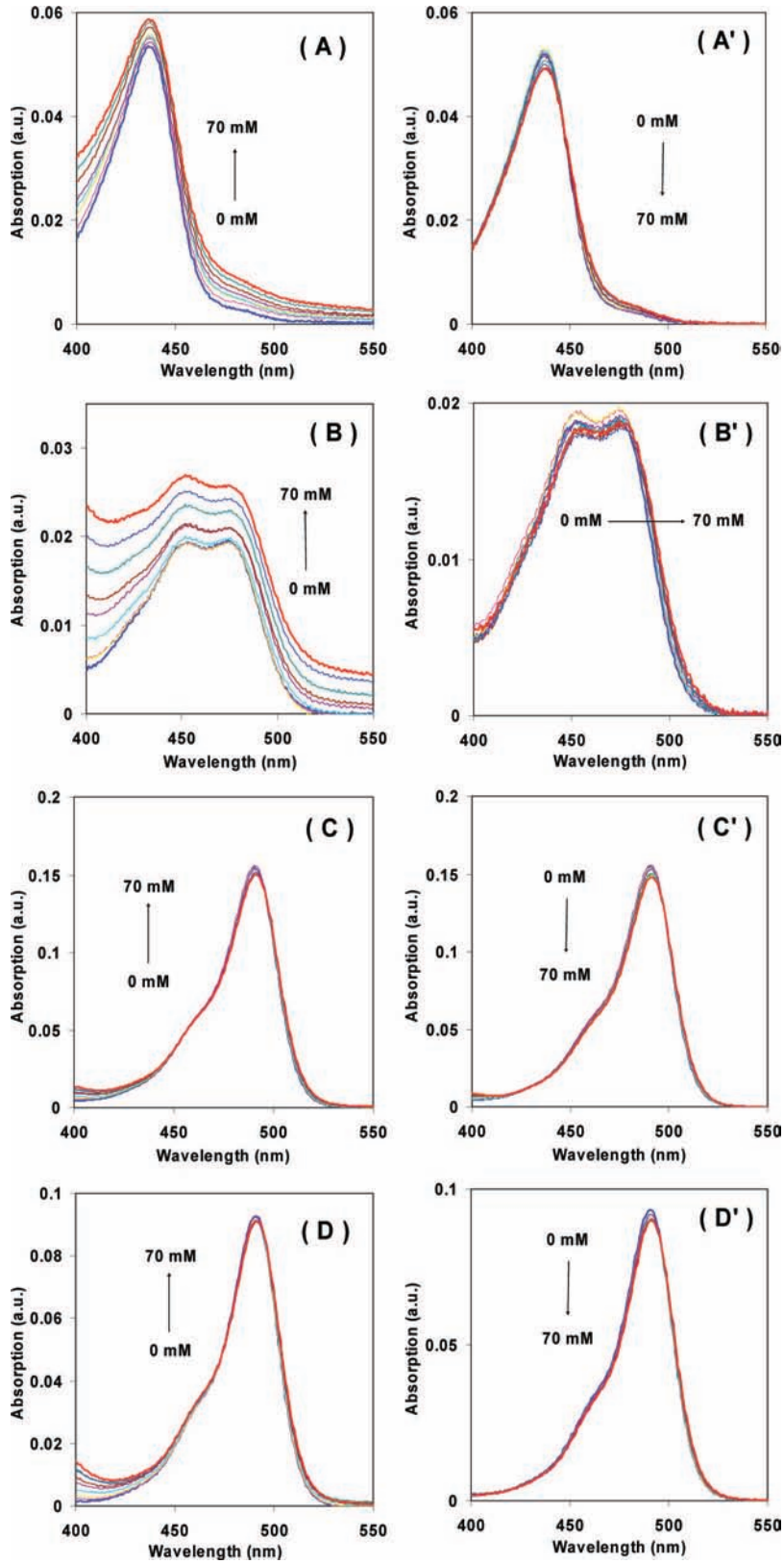

Figure 2. Absorption spectra for FDAH with various concentrations of TrpA and AcTrp in buffered solutions at pH 2.0 (A, A′), pH 5.0 (B, B′), pH 7.4 (C, C′), and pH 11.0 (D, D′). The prime superscript denotes the corresponding corrected absorption spectra (text).

spectra used were acquired under different buffers and ionic strength conditions. Using the ratio of the integrated areas, one can estimate the monoanion contribution to the fluorescence spectrum at pH 5.0 as being approximately 83%. The lifetime data is a little ambiguous because fitting of a biexponential model only shows a slight improvement relative to a monoexponential model, and it was very difficult to reach a real solution when all the parameters are left free to adjust. When the fluorescence decay of fluorescein at pH 5.0 is fitted with a biexponential decay law function, using a fixed $\tau_1 = 4.00$ ns decay time, a second decay time, $\tau_2 = 3.37$ ns, with a 77% intensity contribution is recovered. The two factors, which may

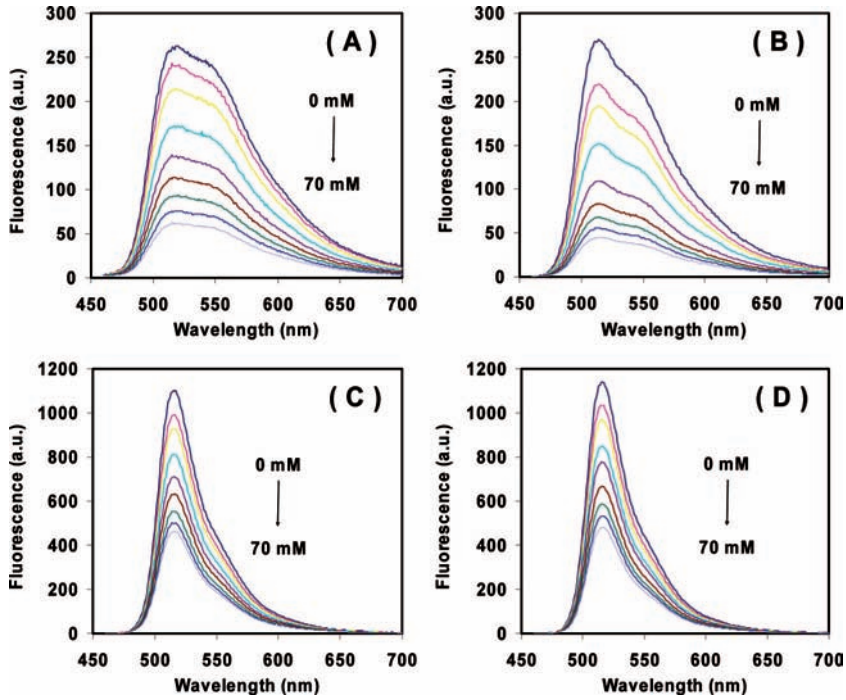

Figure 3. Fluorescence spectra for FDAH with varying TrpA and AcTrp concentrations at pH 2.0 (A), pH 5.0 (B), pH 7.4 (C), and pH 11.0 (D) in buffered solutions.

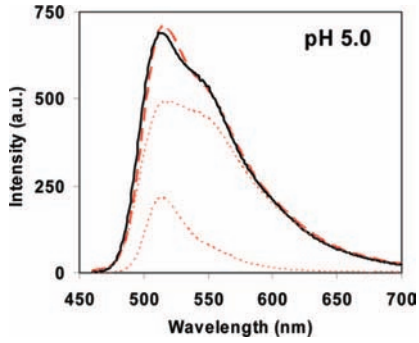

Figure 4. Fluorescence spectra of fluorescein using 450 nm excitation (solid line) at pH 5.0 and recovered fluorescence spectra (dashed line) by multilinear correlation of fluorescence spectra of fluorescein in pH 2.0 and pH 11.0 solutions. The dotted line spectra show the relative contributions of the pH 2.0 and pH 11.0 fluorescence spectra of fluorescein to the total fluorescence spectrum at pH 5.0.

be responsible for the difficulty in obtaining an accurate biexponential fit, are the small difference between the two decay times (τ_1 and τ_2) and the time resolution of the equipment.[28] The lifetime obtained using a single exponential fitting, 3.51 ns, is the same value as the average lifetime value from biexponential fit model. Therefore, for the analysis of the quenching experiments at pH 5.0, a single exponential model was used.

3.4. FDAH Fluorescence Quenching by Tryptophan Derivatives. The Stern−Volmer plots using the quantum yield ratios of FDAH against TrpA and AcTrp concentration shows an upward curvature at all pHs studied (Figure 5) indicating a combination of dynamic and static quenching.[29] In the quenching experiments at pH 2.0 and 5.0 and with TrpA concentrations above 40 mM, the intensity decays are no longer well fitted by a single exponential function because of a fluorescence contribution of TrpA to the total emission. The fluorescence decays for buffered solutions of pure TrpA measured at 520 nm require a triexponential model (0.32, 1.63, and 5.23 ns for pH 2.0; 0.33, 1.77, and 4.98 ns for pH 5.0). Therefore, in the quenching experiments where the concentration of quencher was greater than 40 mM, the TrpA contributed a minor component (<15%) to the total fluorescence decay measured at 520 nm. When AcTrp was used as a quencher, no extra contribution from the quencher fluorescence was observed in the fluorescence decays. In contrast to steady-state results, the ratio values of lifetime without and with quencher (τ_0/τ) show a linear trend with TrpA and AcTrp concentrations (Figure 5). This is because of a dynamic quenching contribution to FDAH excited-state quenching by TrpA and AcTrp. Furthermore, the presence of more than one fluorescent species does not affect the linearity of the dynamic quenching.

No evidence for protolytic equilibrium between the fluorescein monoanion and dianion in the excited-state was found in our study. However, the excited-state monoanion to dianion conversion has been observed in high-concentration phosphate (0.02 to 1 M) or acetate-buffered solutions between pH 6 and 10.[20c,21] In our case, none of the buffers used for any of the measurements had a phosphate anion concentration greater than 10 mM, significantly smaller than the concentration where the protolytic monoanion to dianion equilibrium was observed. If, however, the protolytic equilibrium does occur, we assume (supported by the observation that the fluorescence spectral profiles do not change with the quencher concentration) that it takes place prior to the quenching process.

The decrease in fluorescence quantum yield caused by a combination of collisional, nonfluorescent complex formation, and a sphere-of-action (SOA) quenching mode can be described by the modified Stern−Volmer equation (eq 1):

$$\left(\frac{\Phi_0}{\Phi}\right)\left(\frac{\tau_0}{\tau}\right)^{-1} = (1 + K_{ap}[Q])\exp(V_m[Q]) \qquad (1)$$

$\tau_0/\tau = 1 + K_{SV}[Q]$, where $K_{SV} = k_q \times \tau_0$ (k_q = bimolecular quenching constant, τ_0 = unquenched fluorescence lifetime, and $[Q]$ = quencher concentration). $K_{ap} = \epsilon^* K_C$ where K_C is the

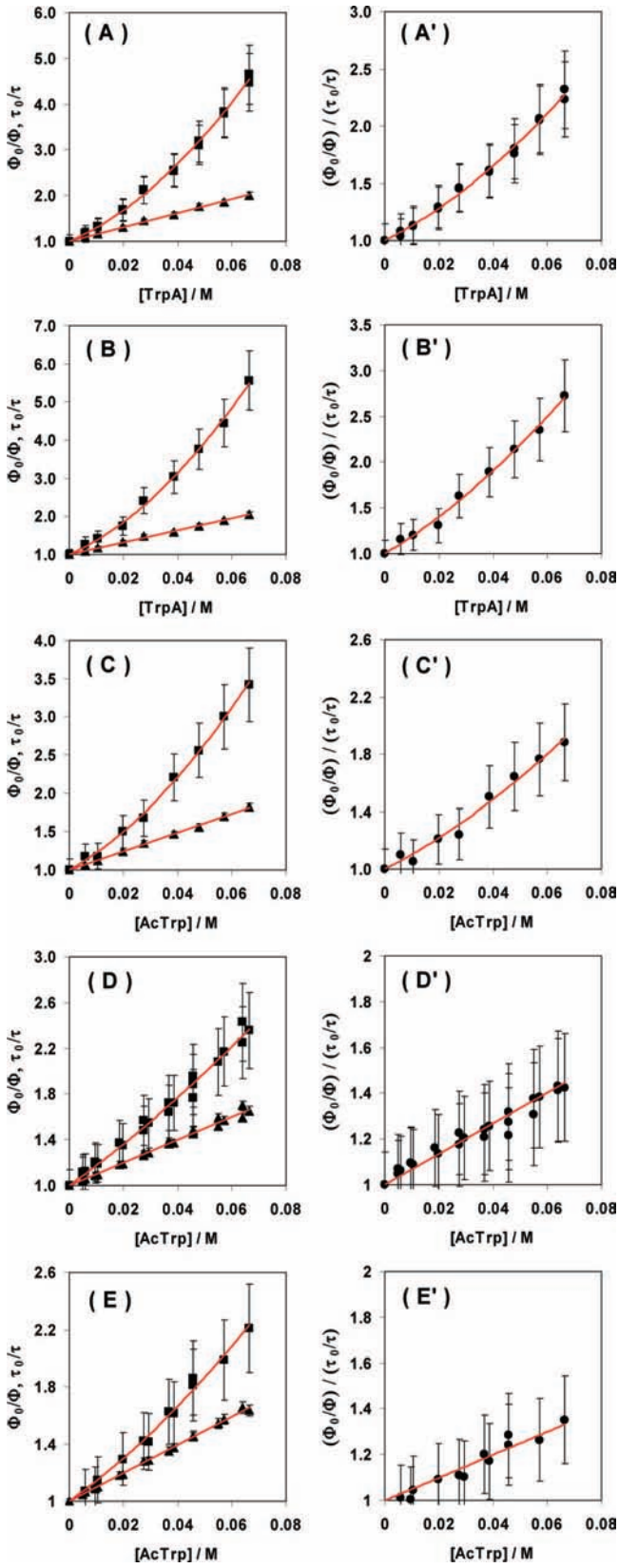

Figure 5. Stern−Volmer plots for FDAH fluorescence quenching by TrpA and AcTrp in buffered solutions at pH 2.0 (A, A′), pH 5.0 (B, B′) and (C, C′), pH 7.4 (D, D′), and pH 11.0 (E, E′). The prime superscript denotes the corresponding Stern−Volmer plots for the ratio between F_0/F and τ_0/τ. The solid square and triangle symbols represent the steady-state and the time-resolved experimental data. All of the solid lines are from the eq 1 fitting model (text). The error bars are calculated using the propagation of errors method for each one of the experimental values.[48]

TABLE 2: Quenching Parameters for Stern−Volmer Plots

quencher	pH	τ_0/ns	K_{sv}/M^{-1}	k_q /10^9 M^{-1} s^{-1}	K_{ap}/M^{-1}	V_m/M^{-1}
TrpA	2.0	2.91	15.3	5.29	3.1	9.6
TrpA	5.0	3.51	15.8	4.50	12.6	5.9
AcTrp	5.0	3.53	12.2	3.46	2.7	7.3
AcTrp	7.4	4.01	10.0	2.52	6.7	—
AcTrp	11.0	4.04	9.9	2.45	5.0	—

complex formation constant, ϵ^* the ratio of molar absorptivities of the complex and the fluorophore at the excitation wavelength,[30] and V_m the molar volume of SOA with a radius:

$$R_{SOA} = \sqrt[3]{\frac{3000V_m}{4\pi N_a}} \quad (2)$$

where, N_a is Avogadro's number. The fitting results are shown in Figure 5 and Table 2.

3.4.1. Static quenching. The nonfluorescent complexes of FDAH are weak as shown by the low values obtained for the apparent equilibrium constants. However, the degree of complex formation in solution is sufficient to cause the curvature observed in the Stern−Volmer plots. The curvature is more pronounced at pH 2.0 and 5.0 because two distinct static processes are present − complex formation and SOA. Marmé et al. [16] have also observed a nonfluorescent complex between fluorescein and tryptophan at pH 7.4, which has an association constant value approximately double the value determined in the FDAH case. We believe that the differences observed are due to the different excitation wavelengths used because the apparent complex association constant depends on the absorption coefficients, which are wavelength dependent. The V_m values (Table 2) are found by fitting eq 1 to the Stern−Volmer experimental data (parts A'−E' of Figure 5), whereas the R_{SOA} values are calculated using eq 2. The respective values for TrpA at pH 2.0 and 5.0 and for AcTrp at pH 5.0 are 15.6 Å, 13.2 Å, and 14.3 Å, whereas no SOA is obtained for pH 7.4 and 11.0. These R_{SOA} values are smaller than those obtained by Doose et al. (∼19 Å), where the Oxazine MR121 fluorophore was used.[18] The R_{SOA} values obtained are reasonable for an energy transfer quenching process, but this mechanism can be ruled out due to the very poor overlap between the donor fluorescence and acceptor absorption. The rate of electron transfer (k_{et}) estimated for a separation distance of ∼14 Å is very low with respect to the time scale of the static quenching process.

Doose et al. point out that probability of electron transfer at distances of ∼19 Å is very low; however, they suggested that a potential long-range attractive interaction between the fluorophore and tryptophan (within ∼20 Å) could influence the relative geometrical arrangement, enhancing quenching beyond the diffusion time scale, which would result in an SOA contribution to the static quenching process.[17,18] Castanho and Prieto[31] suggested that if the time resolution of the fluorescence lifetime measurement was ∼0.5 ns, then the SOA can be interpreted as the sphere of radius R_s, within which the fluorophore can randomly move during that time resolution limit. This means that nonexponential fluorescence decays[29,31] that are commonly observed in transient effects in the diffusional quenching process can be simplified to a single exponential decay. R_s can be calculated by the simple expression:

$$R_S = \sqrt{\frac{5}{3}Dt} \quad (3)$$

SCHEME 2: Quenching Mechanism for Excited Fluorescein Monoanion and Dianion Prototropic Forms

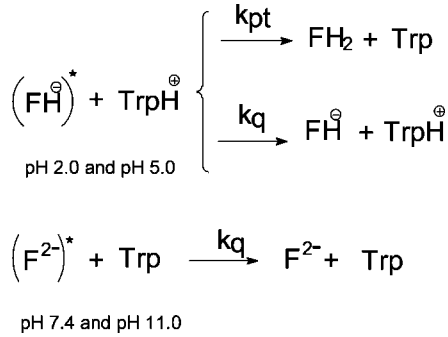

where D is the mutual diffusion constant of the fluorophore and the quencher molecules and t is the time interval for the random walk. If $D = 2 \times 10^{-9}$ m^2s^{-1} [18,29,32]and $t = 0.5$ ns,[28] then $R_s = 12.9$ Å. This shows that fluorescence quenching by diffusional collision that occurs within a sphere of radius 12.9 Å can be considered to be instantaneous. Because $R_s \sim R_{SOA}$, the electron transfer mechanism can still be used to explain the instantaneous static fluorescence quenching in a bimolecular collisional process.

The curvature in the Stern−Volmer plots are small at pH 7.4 (part D of Figure 5) and 11.0 (part E of Figure 5), and, as a consequence, a straight line fits the combined experimental data (parts D' and E' of Figure 5). This indicates that one of the static quenching processes has a very small or negligible contribution to the overall static quenching. We propose that it is the sphere-of-action that can be eliminated because spectroscopic evidence shows complex formation at pH 7.4 and 11.0. However, we would also expect that the random walk based SOA quenching (within the equipment time resolution) should be present at pH 7.4 and 11.0. This inconsistency indicates that a different process operates under neutral or basic conditions compared to acidic environments.

Assuming that the fluorescence quantum yield is zero for the neutral form[20b,22b,c] or that protonation may lead to the nonfluorescent zwitterionic[20a] or lactone forms,[33] then protonation of the excited monoanion can be considered as a quenching process (Scheme 2). The TrpA species at pH 2.0 and 5.0, and AcTrp species at pH 5.0, are probably protonated and so can transfer a proton to the monoanionic FDAH. The protonation of the monoanion to the neutral form can occur within the diffusional rate limit with values $\sim 5.4 \times 10^{10}$ $M^{-1}s^{-1}$.[21b] If one considers the local tryptophan derivative concentration (V_m in Table 1), the time required for a proton transfer within the R_{SOA} distance is less than 5 ps ($1/(5.4 \times 10^{10}\ V_m)$) approximately, or $k_{pt} > 2 \times 10^{11}$ s^{-1}, then protonation of the monoanion can be considered as instantaneous within the instrument time resolution. The protonation can be even faster if hydrogen bonding networks in the solvation layers connecting the fluorophore and the quencher molecules are involved in the proton transfer.[34] If, however, the rate of the neutral species formation by protonation is not fast enough, then the reverse reaction to the excited monoanion can be competitive. In this case, a mechanism that involves both proton and electron transfer (proton-coupled electron transfer)[35] cannot be ruled out. In any case, the same process is more difficult in alkaline media due to the lack of a labile proton from the quencher molecule. Further experiments using better time resolution instrumentation, changing viscosity, or the kinetic isotopic effect can help determine if the proton transfer (or coupled with electron transfer) is relevant to the static contribution to the whole quenching process.

3.4.2. Dynamic quenching. The k_q values show a clear decrease when the pH increases, and the value for pH 7.4 is in agreement with the bimolecular rate constant obtained by Marmé et al. using L-tryptophan as the fluorescein quencher.[16] The bimolecular quenching process can be represented by the encounter controlled reaction mechanism[36] (Scheme 3) and k_q can be calculated from:

$$k_q = \frac{k_{et}k_d}{k_{-d} + k_{et}} \tag{5}$$

where k_d is the diffusion rate constant, k_{-d} the dissociation rate constant for the diffusional encounter pair, and k_{et} is the electron transfer reaction rate constant. k_d can be calculated using the Debye−Smoluchoswski model for diffusion of ions[27,37] (eq 6):

$$k_d = \frac{2N_a k_B T}{3000\eta}\left(\frac{R_F}{R_T} + \frac{R_T}{R_F} + 2\right) \frac{1}{R_{FT}\int_{R_{FT}}^{\infty} r^{-2}\exp[w(r,I)/k_B T]dr} \tag{6}$$

k_B is the Boltzmann constant, T is the temperature, η is the water viscosity (0.91 cP at 25 °C), and R_F and R_T are the hard sphere radii of the FDAH and the tryptophan derivatives, where $R_{FT} = R_F + R_T$. The $R_F = 4.4$ Å, and $R_T = 4.2$ Å for AcTrp, and $R_T = 3.8$ Å for TrpA.[38] I is the ionic strength of solution, and $w(r,I)$ is the work function for the charged reactants at the separation distance r in the presence of an ionic atmosphere based on ionic strength I calculated by eq 7:

$$w(r,I) = \frac{z_F z_T e^2}{2\varepsilon r}\left[\frac{\exp(\beta\sigma_F)}{1+\beta\sigma_F} + \frac{\exp(\beta\sigma_T)}{1+\beta\sigma_T}\right]\exp(-\beta r) \tag{7}$$

where $\beta = [(8\pi N_a e^2)/(1000\varepsilon k_B T)]^{1/2}$, $z_F z_T$ is the ionic reactants charge product and ε is the static dielectric constant of water at 25 °C ($\varepsilon = 78.3$), e is the electron charge, σ_F and σ_T are the radii of the respective reagent molecule plus the radius of the dominant counterion in the ionic atmosphere. In this work, we assume that the contributions of the counter-ions to the total size of fluorophore and quencher molecules are small. Therefore, σ_F and σ_T are assumed to be R_F and R_T, respectively. The k_{-d} is calculated by using the Eigen treatment for the dissociation of ionic encounter pair (eq 8):

$$k_{-d} = \frac{k_B T}{2\pi\eta R_{FT}^2}\left(\frac{1}{R_F} + \frac{1}{R_T}\right)\frac{\exp[w(R_{FT},I)/k_B T]}{R_{FT}\int_{R_{FT}}^{\infty} r^{-2}\exp[w(r,I)/k_B T]dr} \tag{8}$$

The diffusion parameters can be calculated by using a numerical integration (Simpson method) of eqs 6 and 8 over the limit from R_{FT} to 5000 Å.

SCHEME 3: Bimolecular Fluorescence Quenching Mechanisms

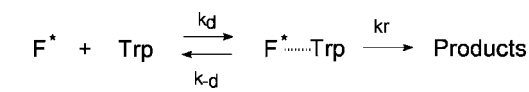

TABLE 3: Diffusion Rate Constant, Diffusion Dissociation Rate Constants, and Electron Transfer Rate Constants Extracted from FDAH Fluorescence Dynamic Quenching Parameters

pH	$z_F z_T$	$k_d/10^9$ M^{-1} s^{-1}	$k_{-d}/10^9$ s^{-1}	$k_{el}/10^9$ s^{-1}	$-\Delta G$ °/eV	H_{FT}/cm^{-1}
2.0	(−1).(+1)	8.48−8.18	3.92−4.12	6.23−6.67	0.59	25.1
5.0	(−1).(+1)	7.83−7.77	4.45−4.52	6.19−6.07	0.67	17.0
5.0[a]	(−1).(0)	7.36	4.59	4.08−3.99	0.67	11.6
7.4	(−2).(0)	7.36	4.59	2.45−2.30	0.62	9.6
11.0	(−2).(−1)	5.78−6.36	7.27−6.53	4.72−4.53	0.86	5.7

[a] AcTrp was used as the quencher.

In the excited state, the dianion is dominant at pH 7.4 and 11.0, whereas at pH 2.0 and 5.0 the monoanion is the major species. For the quencher, charges were assumed to be single positive (+1) for TrpA at pH 2.0 and 5.0, zero for AcTrp at pH 5.0, and 7.4, and single negative (−1) at pH 11.0 for AcTrp. It is important to note that the ionic strength of buffer solutions used in these quenching experiments was relatively high (>0.2 M). Therefore, when the additional ionic strength contribution due to the quenchers was taken into account in the k_d and k_{-d} calculations, a small variation in the k_d and k_{-d} values was obtained (Table 3). Furthermore, depending on the sign and magnitude of charges that are present in the fluorophore and quencher, the diffusion reaction can be accelerated or retarded. The electrostatic interaction also explains the hindered dissociation of the encounter pair in acid media, where the encounter pair is composed of species with opposite charges, whereas in alkaline media dissociation is enhanced by the repulsion between the ions of same charge.

The k_{et} values can be recovered from k_q using eq 5. The k_{et} values are most likely due to a photoinduced electron transfer between tryptophan acting as an electron donor to the fluorescein molecule. We can assess the k_{et} value using the rate constant electron-transfer reactions from semiclassic and nonadiabatic description from Marcus theory:[39]

$$k_{et} = \frac{4\pi^2 H_{FT}^2}{h(4\pi\lambda k_B T)^{\frac{1}{2}}} \exp\left[-\frac{(\lambda + \Delta G^0)^2}{4\lambda k_B T}\right] \qquad (9)$$

where h is Planck's constant, H_{FT} is the electronic coupling coefficient related to vibration, distance, and orientation of the reacting species, and λ, the reorganization energy, which has motion contributions from the atoms of the reactants and the solvent reorganization free energy in an ionic atmosphere situation. ΔG^0 is the driving force of the reaction[40] determined by the redox potentials of the FDAH, $E^0(A/A^{-\bullet})$, in the excited-state at vibrational zero electronic level (additional $\Delta E_{0,0}$ energy), and the tryptophan derivatives, $E^0(D^{+\bullet}/D)$, plus the work terms $w(D^{+\bullet}A^{-\bullet}) - w(D\,A)$, that is:

$$\Delta G^0 = E^0(D^{+\bullet}/D) - E^0(A/A^{-\bullet}) + w(D^{+\bullet}A^{-\bullet}) - w(DA) - \Delta E_{0,0} \qquad (10)$$

The Coulombic interaction experienced by the reactants and products as they are brought together in the encounter pair are included in eq 10 as being $w(D\,A)$ and $w(D^{+\bullet}A^{-\bullet})$, respectively, and calculated using eq 7.

The redox potential used in the k_{et} calculation can be obtained from electrochemical data accessible in the literature. Using results from Tommos et al.,[41] the $E^0[Trp^{+\bullet}/Trp]$ versus NHE are 1.07, 0.99, 0.88, and 0.64 V at pH 2.0, 5.0, 7.4, and 11.0, respectively. In the case of the fluorescein dianion, the reduction potential $E^0[F^{2-}/F^{3-\bullet}] = 0.91$ V versus NHE[42] was used. The monoanionic reduction potential, $E^0[FH^-/FH^{2-\bullet}]$, can be estimated following Compton et al.'s suggestion[43] to use the pK_a values of FH^- to $FH^{2-\bullet}$ (6.68[23] and 9.5,[44] respectively) and the reduction potential of F^{2-} to $F^{3-\bullet}$. Applying the Nernst general equation for an equilibrium situation, $E^0[FH^-/FH^{2-\bullet}] = 0.74$ V versus NHE is found. Finally, the total reduction potential for the electron acceptor center has to be added to the excited single-state energy (E_S) of 2.40 eV for both prototropic forms (monoanion and dianion) because both have approximately the same fluorescence maximum ~515 nm observed in all of the buffer conditions used. The electron transfer driven forces for diffusional encounter pairs: $FDAH^{-1}/TrpA^{+1}$ (pH 2.0), $FDAH^{-1}/TrpA^{+1}$ (pH 5.0), $FDAH^{-1}/AcTrp^0$ (pH 5.0), $FDAH^{-2}/AcTrp^0$ (pH 7.4), and $FDAH^{-2}/AcTrp^{-1}$ (pH 11) using the above values are shown in the Table 3.

Götz et al.[45] applied femtosecond absorption spectroscopy to show that fluorescein is electron photoreduced by either tryptophan or tyrosine after binding to Anticalin, a Lipocalin protein, where the fluorescein trianion radical is formed very quickly in about 400 fs. The ΔG^0 value used by Götz et al. is in the same range as found in our work.

The solvent reorganization energy, λ_s, can be calculated (eq 11) using the dielectric continuum model of Marcus,[46] where n is the refraction index of the solvent and the rest of the parameters having been defined previously:

$$\lambda_S = \frac{e^2}{4\pi\varepsilon_0}\left(\frac{1}{2R_F} + \frac{1}{2R_T} - \frac{1}{R}\right)\left(\frac{1}{n^2} - \frac{1}{\varepsilon}\right) \qquad (11)$$

Electron transfer may occur when the molecules are close to each other, and then the dynamics of reaction are strongly dependent on the separation distance. For a contact distance of $R = R_{FT}$, then $\lambda_S \sim 0.96$ eV for TrpA and ~0.92 eV for AcTrp. The internal reorganization energy used by our calculation is the same one estimated by Götz et al.,[45] which is equal to 0.42 eV. Therefore, the total reorganization energy λ, which is equal to the solvent reorganization energy plus the internal reorganization energy, is 1.34 eV for AcTrp and 1.40 eV for TrpA.

Combining the electron transfer eq 9 and the diffusional rate equations (eqs 6 and 8), with eq 5, and using the reasonable parameters mentioned above, the electronic coupling H_{ab} can be calculated from the experimental value k_q. As noted in Table 3, the driving force increases ($-\Delta G^0$) in the opposite direction to that of the electron transfer rate, as a result of decreasing electronic coupling between the ionic species. This indicates that a spatial reconfiguration between the reaction centers may be necessary to promote more efficient electron transfer; however, the electrostatic interaction between the quencher and fluorophore may prevent the system from reaching this ideal geometrical configuration. For example, in an investigation of photoinduced electron transfer in fluorescein, Miura et al. found a very small coupling (7.0 cm^{-1}) despite both quencher and

fluorophore being covalently bound.[47] They suggest that the carboxylic group prevents free rotation between the donor and acceptor centers giving the centers an orthogonal orientation. In the case of charged FDAH and tryptophan derivatives, we propose that molecular repulsion may prevent the necessary geometrical alignment required to provide better coupling. However, if the electrostatic interaction is attractive, it would provide a better alignment of the donor and acceptor centers, and thus improve the coupling. For comparison, the values for the electronic coupling obtained here (Table 3) are around 20-fold smaller than the electronic coupling between the fluorescein and tryptophan in the Anticalin protein.[45] In the Anticalin protein, the electron transfer is assumed to be barrierless and therefore the reorganization energy is taken to be the same value as that of the driving force. Nevertheless, in the Anticalin case, fluorescein is located in the pocket where the geometrical arrangement is appropriate for a very efficient electron transfer process. Therefore, the electronic coupling in the Anticalin case reaches a maximum value at the closest distance between the reaction centers. To validate the electronic coupling of FDAH and tryptophan in the diffusional encounter pair (Table 3), we can apply the distance dependent electronic coupling under the same assumptions applied to the Anticalin case by using eq 12.

$$H_{FT}^2 = H_{FT,0}^2 \exp[-\beta(R - R_0)] \qquad (12)$$

where $H_{FT,0}$ is the electronic coupling matrix element for a donor−acceptor pair at van der Waals separation R_0, and β is a decay constant scaling the electronic coupling and R the encounter distance between quencher and fluorophore. If we take typical values of 3.5 Å for a coplanar distance between fluorescein and tryptophan centers,[45] 1−1.65 Å as the β value,[39,45] 170 cm^{-1} for the $H_{FT,0}$ coupling found in the Anticalin case,[45] then the H_{FT} coupling is in the range 2.5−16.2 cm^{-1} for AcTrp and TrpA when the same $R = R_{FT}$ distance is used for the above calculations and after applying eq 12. In other words, the coupling in the encounter complex is similar to that observed in Anticalin, with respect to the electronic coupling distance dependence.

4. Conclusions

Fluorescein is a very widely used fluorescent label in biological science; however, the factors that may affect the intensity of its fluorescence when bioconjugated are not fully understood. In this work, we have shown that the fluorescence of fluorescein, at different pH, in the presence of tryptophan is a very complex process. Absorption spectroscopy data and Stern−Volmer analyses show the presence of nonfluorescent, fluorescein−tryptophan complexes at all pHs studied. In the static quenching process, sphere-of-action (SOA) is also clearly present in acidic media (pH 2.0 and 5.0), whereas in alkaline media, SOA is not observed in the range of tryptophan concentrations (<70 mM) used in this study. We surmise that the difference in mechanisms is due to proton transfer from the quencher molecules that enhance the SOA in acid media. In the dynamic quenching process, electron transfer parameters were determined at all of the pHs studied. The electronic coupling between the main prototropic species and the indole-based molecules TrpA and AcTrp show some dependence on the net charge involved in the formation of diffusion paired complexes, which can dictate the spatial organization between the reaction centers for electron transfer. Therefore, changes in fluorescence intensity and lifetime of the fluorescein in a labeled protein should not be directly correlated only to the external factors when amino acids such as tryptophan are located close to the conjugated probe.

Acknowledgment. This work was supported by funding from a Science Foundation Ireland Principal Investigator Grant (number 02/IN.1/M231 to A.G.R.) and the National Biophotonics Imaging Platform, an Irish Higher Education Authority Programme for Research in Third Level Institutions supported project.

References and Notes

(1) Giepmans, B. N. G.; Adams, S. R.; Ellisman, M. H.; Tsien, R. Y. *Science* **2006**, *312*, 217–224.
(2) Slavik, J. *Fluorescence Probes in Cellular and Molecular Biology*; CRC Press: Boca Raton, 1994.
(3) Wallrabe, H.; Periasamy, A. *Curr. Opin. Biotech.* **2005**, *16*, 19–27.
(4) Kim, S. A.; Heinze, K. G.; Schwille, P. *Nature Methods* **2007**, *4* (11), 963–973.
(5) Togashi, D. M.; Ryder, A. G. *Exp. Mol. Pathol.* **2007**, *82* (2), 135–141.
(6) Tsien, R. Y.; Waggoner, A. *Handbook of Biological Confocal Microscopy*, 3rd ed.; Pawley J. B., Ed.; Plenum Press: New York, 2006; pp 338−356.
(7) Waggoner, A. *Curr. Opin. Chem. Bio.* **2006**, *10* (1), 62–66.
(8) Togashi, D. M.; Ryder, A. G. *J. Fluoresc.* **2006**, *16*, 153–160.
(9) Togashi, D. M.; Ryder, A. G. *J. Fluoresc.* **2008**, 519–526.
(10) Andrade, S. M.; Costa, S. M. B. *Biophys. J.* **2002**, *82* (3), 1607–1619.
(11) Carvell, M.; Robb, I. D.; Small, P. W. *Polymer* **1998**, *39* (2), 393–398.
(12) Deka, C.; Lehnert, B. E.; Lehnert, N. M.; Jones, G. M.; Sklar, L. A.; Steinkamp, J. A. *Cytometry* **1996**, *25*, 271–279.
(13) Sparano, B. A.; Shahi, S. P.; Koide, K. *Org. Lett.* **2004**, *6* (12), 1947–1949.
(14) Klonis, N.; Sawyer, W. H. *Photochem. Photobiol.* **2003**, *77* (5), 502–509.
(15) Hungerford, G.; Benesch, J.; Mano, J. F.; Reis, R. L. *Photochem. Phobiol. Sci.* **2007**, *6*, 152–158.
(16) Marmé, N.; Knemeyer, J.-P.; Sauer, M.; Wolfrum, J. *Bioconjugate Chem.* **2003**, *14*, 1133–1139.
(17) Vaiana, A. C.; Neuweiler, H.; Schulz, A.; Wolfrum, J.; Sauer, M.; Smith, J. C. *J. Am. Chem. Soc.* **2003**, *125*, 14564–14572.
(18) Doose, S.; Neuweiler, H.; Sauer, M. *ChemPhysChem.* **2005**, *6*, 2277–2285.
(19) Szollosi, J.; Damjanovich, S.; Matyus, L. *Cytometry* **1998**, *34* (4), 159–179.
(20) (a) Klonis, N.; Sawyer, W. H. *J. Fluoresc.* **1996**, *6* (3), 148–157. (b) Sjöback, R.; Nygren, J.; Kubista, M. *Spectrochim. Acta, Part A* **1995**, *51* (6), L7−L21. (c) Ygureabide, J.; Talavera, E.; Alvarez, J. M.; Quintero, B. *Photochem. Photobiol.* **1994**, *60* (5), 435–441. (d) Marting, M. M.; Lindqvist, L. *J. Lumin.* **1975**, *10*, 381–390.
(21) (a) Alvarez-Pez, J. M.; Ballesteros, L.; Talavera, E.; Yguerabide, J. *J. Phys. Chem. A* **2001**, *105*, 6320–6332. (b) Orte, A.; Crovetto, L.; Talavera, E. M.; Maçanita, A. L.; Orte, J. C.; Alvarez-Pez, J. M. *J. Phys. Chem. A* **2005**, *109*, 8705–8718.
(22) (a) Diehl, H.; Markuszewski, R. *Talanta* **1989**, *36* (3), 416–418. (b) Rozwadowski, M. *Acta Phys. Pol.* **1961**, *20*, 1005–1017. (c) Leonhardt, H.; Gordon, L.; Livingston, R. *J. Phys. Chem.* **1971**, *75* (2), 245–249.
(23) Smith, S. A.; Pretorius, W. A. *WATER SA* **2002**, *28* (4), 395–402.
(24) The ionic strengths were calculated by the salt composition provided by the supplier. For pH 11, the ionic strength was estimated by determining the amount of chloride by gravimetric analysis.
(25) Boens, N.; Qin, W. W.; Basaric, N.; Hofkens, J.; Ameloot, M.; Pouget, J.; Lefevre, J. P.; Valeur, B.; Gratton, E.; Vandeven, M.; Silva, N. D.; Engelborghs, Y.; Willaert, K.; Sillen, A.; Rumbles, G.; Phillips, D.; Visser, A. J. W. G.; van Hoek, A.; Lakowicz, J. R.; Malak, H.; Gryczynski, I.; Szabo, A. G.; Krajcarski, D. T.; Tamai, N.; Miura, A. *Anal. Chem.* **2007**, *79*, 2137–2149.
(26) (a) Chen, S.-N.; Hoffman, Z. *J. Phys. Chem.* **1974**, *78*, 21–2099. (b) *The Merck Index*, 14th ed.; O'Neil, M. J., Ed.; Merck Research Laboratories: NJ, 2006; p 1682.
(27) Togashi, D. M.; Costa, S. M. B. *New J. Chem.* **2002**, *26*, 1774–1783.
(28) Approximate fwhm of the instrument response function (IRF) = ~500 ps.
(29) Lakowicz, J. R. *Principles of Fluorescence Spectroscopy*, 3rd ed.; Springer: Singapore, 2006; Ch. 8.

(30) Costa, S. M. B.; López-Cornejo, P.; Togashi, D. M.; Laia, C. A. T. *J. Photochem. Photobiol. A* **2001**, *142* (2−3), 151–161.

(31) Castanho, M. A. R. B.; Prieto, M. J. E. *Biochim. Biophys. Acta* **1998**, *1373*, 1–16.

(32) Culbertson, C. T.; Jacobson, S. C.; Ramsey, J. M. *Talanta* **2002**, *56*, 365–373.

(33) Kobayashi, T.; Urano, Y.; Kamiya, M.; Ueno, T.; Kojima, H.; Nagano, T. *J. Am. Chem. Soc.* **2007**, *129*, 6696–6697.

(34) Mezer, A.; Friedman, R.; Noivirt, O.; Nachliel, E.; Gutman, M. *J. Phys. Chem. B* **2005**, *109*, 11379–11388.

(35) (a) Huynh, M. H. V.; Meyer, T. J. *Chem. Rev.* **2007**, *107*, 5004. (b) Mayer, J. M. *Annu. Rev. Phys. Chem.* **2004**, *55*, 363.

(36) (a) Truhlar, D. G. *J. Chem. Educ.* **1985**, *62* (2), 104–106. (b) Calef, D. F.; Deutch, J. M. *Annu. Rev. Phys. Chem.* **1983**, *34*, 493–524.

(37) Chiorboli, C.; Indelli, M. T.; Scandola, M. A. R.; Scandola, F. *J. Phys. Chem.* **1988**, *92*, 156–163.

(38) The molecular radii were estimated from the calculation of the molar volumes of studied molecules using Molecular model *ACD/ChemSketch* Version 5.12 (2002).

(39) (a) Marcus, R. A. *J. Chem. Phys.* **1956**, *24*, 966–978. (b) Closs, G. L.; Miller, J. R. *Science* **1988**, *240*, 440–447. (c) Barbara, P. F.; Meyer, T. J.; Ratner, M. A. *J. Phys. Chem.* **1996**, *100* (13), 13148–13168.

(40) Although the IUPAC recommendation for the Gibbs energy of photoinduced electron transfer units is $J \cdot mol^{-1}$, we are using electronvolts (eV) to facilitate comparison with other reported data.

(41) Tommos, C.; Skalicky, J. J.; Pilloud, D. L.; Wand, A. J.; Dutton, P. L. *Biochemistry* **1999**, *38*, 9495–9507.

(42) Compton, R. G.; Manson, D.; Unwin, P. R. *J. Chem. Soc., Faraday Trans. 1* **1988**, *84*, 2057–2068.

(43) Compton, R. G.; Mason, D.; Unwin, P. R. *J. Chem. Soc., Faraday Trans. 1* **1988**, *84* (2), 483–489.

(44) Cordier, P.; Grossweiner, L. I. *J. Phys. Chem.* **1968**, *72* (6), 2018–2026.

(45) Gotz, M.; Hess, S.; Beste, G.; Skerra, A.; Michel-Beyerle, M. E. *Biochemistry* **2002**, *41*, 4156–4164.

(46) Clark, C. D.; Hoffman, M. Z. *Chem. Rev.* **1997**, *159*, 359–373.

(47) Miura, T.; Urano, Y.; Tanaka, K.; Nagano, T.; Ohkubo, K.; Fukuzumi, S. *J. Am. Chem. Soc.* **2003**, *125*, 8666–8671.

(48) Steinfeld, J. I.; Francisco, J. S.; Hase, W. L. *Chemical Kinetics and Dynamics*, 2nd ed.; Prentice Hall: NJ, 1999; p 108.

JP808121Y